University of Pennsylvania
ScholarlyCommons

Departmental Papers (MSE) | Department of Materials Science & Engineering

February 2001

Analysis of phase distributions in the $Li_2O–Nb_2O_5–TiO_2$ system by piezoresponse imaging

Albina Y. Borisevich
University of Pennsylvania

Sergei V. Kalinin
University of Pennsylvania

Dawn A. Bonnell
University of Pennsylvania, bonnell@lrsm.upenn.edu

Peter K. Davies
University of Pennsylvania, davies@lrsm.upenn.edu

Follow this and additional works at: http://repository.upenn.edu/mse_papers

Recommended Citation

Borisevich, A. Y., Kalinin, S. V., Bonnell, D. A., & Davies, P. K. (2001). Analysis of phase distributions in the $Li_2O–Nb_2O_5–TiO_2$ system by piezoresponse imaging. Retrieved from http://repository.upenn.edu/mse_papers/58

Copyright Materials Research Society. Reprinted from *Journal of Materials Research*, Volume 16, Issue 2, February 2001, pages 329-332.
Publisher URL: http://www.mrs.org/publications/jmr/

This paper is posted at ScholarlyCommons. http://repository.upenn.edu/mse_papers/58
For more information, please contact repository@pobox.upenn.edu.

Analysis of phase distributions in the $Li_2O–Nb_2O_5–TiO_2$ system by piezoresponse imaging

Abstract
The *M*-phase solid solutions $Li_{1+x-y}Nb_{1-x-3y}Ti_{x+4y}O_3$) ($0.1 \leq x \leq 0.3$, $0 \leq y \leq 0.175$) in the $Li_2O–Nb_2O_5–TiO_2$ system have promising microwave dielectric properties. However, these compounds can contain small quantities of ferroelectric impurities that affect the polarization response of the material. Due to their low concentration and their chemical similarity to the host material, the impurities cannot be detected by x-ray diffraction or local elemental analysis. Scanning surface potential microscopy and piezoresponse imaging were used to analyze phase compositions in this system. Piezoresponse imaging demonstrated the presence of thin (<200–300 nm) ferroelectric layers on the grain boundaries oriented along the *c*-axis of the *M*-phase. Differences between the surface potential and the piezoresponse of ferroelectric multicomponent systems are discussed.

Comments
Copyright Materials Research Society. Reprinted from *Journal of Materials Research*, Volume 16, Issue 2, February 2001, pages 329-332.
Publisher URL: http://www.mrs.org/publications/jmr/

This journal article is available at ScholarlyCommons: http://repository.upenn.edu/mse_papers/58

Analysis of phase distributions in the Li_2O–Nb_2O_5–TiO_2 system by piezoresponse imaging

Albina Y. Borisevich, Sergei V. Kalinin, Dawn A. Bonnell, and Peter K. Davies
Department of Materials Science & Engineering, University of Pennsylvania, 3231 Walnut Street, Philadelphia, Pennsylvania 19104

(Received 16 June 2000; accepted 6 November 2000)

The *M*-phase solid solutions $Li_{1+x-y}Nb_{1-x-3y}Ti_{x+4y}O_3$) ($0.1 \leqslant x \leqslant 0.3$, $0 \leqslant y \leqslant 0.175$) in the Li_2O–Nb_2O_5–TiO_2 system have promising microwave dielectric properties. However, these compounds can contain small quantities of ferroelectric impurities that affect the polarization response of the material. Due to their low concentration and their chemical similarity to the host material, the impurities cannot be detected by x-ray diffraction or local elemental analysis. Scanning surface potential microscopy and piezoresponse imaging were used to analyze phase compositions in this system. Piezoresponse imaging demonstrated the presence of thin (<200–300 nm) ferroelectric layers on the grain boundaries oriented along the *c*-axis of the *M*-phase. Differences between the surface potential and the piezoresponse of ferroelectric multicomponent systems are discussed.

Phase analysis has always been a critical tool for investigations in the fields of solid-state chemistry and inorganic materials. X-ray diffraction (XRD) can be used to resolve different phases in multiphase samples provided that the phases are present in relatively high concentration ($\geqslant$5%). When the nature of small concentrations of impurity phases must be determined, methods of local structural and compositional analysis are used, such as electron diffraction or energy dispersive x-ray spectroscopy (EDX). However, these techniques are not applicable for distinguishing phases with very similar compositions. In these cases properties other than composition or structure must be probed to conduct reliable phase analysis. In this communication we report on the application of piezoresponse imaging and scanning surface potential microscopy for phase analysis in the Li_2O–Nb_2O_5–TiO_2 system.

Phase equilibria in the Li_2O–Nb_2O_5–TiO_2 ternary system were studied in detail by Villafuerte-Castrejon *et al.*[1] Among the many phases described, the so-called "*M*-phase" $Li_{1+x-y}Nb_{1-x-3y}Ti_{x+4y}O_3$ ($0.1 \leqslant x \leqslant 0.3$, $0 \leqslant y \leqslant 0.175$) solid solutions have been shown to be of particular interest because of their promising microwave dielectric properties.[2] Transmission electron microscopy and XRD investigations[3–6] suggest that these phases have complex structures of variable periodicity, formed by the intergrowth of $LiNbO_3$-like blocks with layers of a different structural nature.

Samples within the *M*-phase field were synthesized from dried Li_2CO_3 (Baker, 99.0%), Nb_2O_5 (Cerac, 99.95%), and TiO_2 (Cerac, 99.9%) powders using standard solid-state techniques. Several heatings at 1100 °C were required to produce samples that were single-phase to x-rays. The necessity of multicycle annealing for some compositions suggests that equilibrium in this system is difficult to achieve. This is consistent with the complex character of the *M*-phase structures and is often observed in systems that exhibit long periodicities.

Polarization measurements were performed with a RT-66A ferroelectric test system (Radiant Technologies, Inc., Albuquerque, NM) in virtual ground mode. Although $LiNbO_3$-based solid solutions, which form a phase field adjacent to the *M*-phase region, are well-known ferroelectrics with high remanent polarizations, most of the *M*-phase samples exhibited purely paraelectric behavior. However, some compositions with a low Ti content gave a weak ferroelectric response (approximately 10^{-1}–10^{-2} $\mu C/cm^2$). The value of the remanent polarization varied inconsistently even for different samples of the same composition. The most pronounced effect was observed in $Li_{1.1}Nb_{0.9}Ti_{0.1}O_3$. The shape of the corresponding hysteresis loop was irregular (Fig. 1), suggesting considerable leakage in the system, and it did not saturate for fields up to approximately 60 kV/cm.

It was concluded that all *M*-phase solid solutions are in fact paraelectric and that the weak ferroelectric response in some compositions is caused by a ferroelectric impurity, namely a $LiNbO_3$ solid solution that is not detected by XRD. The magnitude of the observed remanent polarization suggests that the quantities of this second phase are very small (P_r for pure $LiNbO_3$ is 50 $\mu C/cm^2$)[7] and have a small effect on the bulk characteristics of the

 © 2001 Materials Research Society

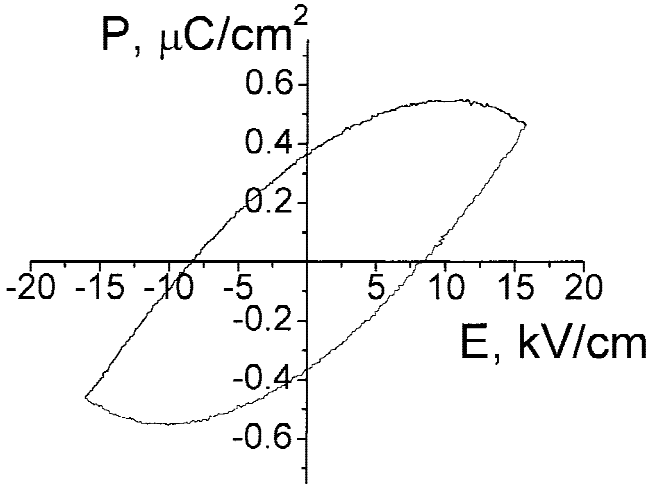

FIG. 1. Typical hysteresis loop for $Li_{1.1}Nb_{0.9}Ti_{0.1}O_3$.

samples. Verification of this conclusion was attempted by local elemental analysis; however, the compositional similarity of the *M*-phases and the $LiNbO_3$ solid solutions prohibited their identification. Because the $LiNbO_3$ solid solution exhibits ferroelectric and piezoelectric properties, while the *M*-phase is paraelectric, successful phase identification was found to be possible using piezoresponse imaging (PRI) and scanning surface potential microscopy (SSPM).

Both SSPM and PRI are force-based SPM techniques that utilize voltage modulation; i.e., during imaging the piezoelectric actuator driving the cantilever is disengaged and a bias is applied directly to a conductive tip. In PRI the tip is brought into contact with the surface and the piezoelectric response of the surface is detected as the first harmonic component of the bias-induced tip deflection. In SSPM the tip is held at a fixed distance above the surface (typically 10–100 nm) and the feedback loop is used to nullify the first harmonic of the electrostatic force between the tip and the surface by adjusting the constant bias on the tip. It is generally assumed that SSPM provides quantitative information on local potentials related to local polarization, adsorbates, etc. Topographic inhomogeneities also strongly influence the potential image.[8] PRI provides information on polarization through the local piezoresponse; however, the contrast in PRI may include contributions from Maxwell stresses,[9] polarization switching below the tip, etc. It should be noted that vast majority of PRI studies were performed on single-phase samples,[10–13] while the potential of this technique for phase analysis of multiphase systems is as yet unexplored. At the same time, SSPM and PRI of multiphase systems can further the understanding of the role of different factors in the imaging mechanism of both techniques.

The atomic force microscopy, SSPM,[14] and piezoresponse measurements were performed on a commercial instrument (Digital Instruments Dimension 3000 NS-III, Santa Barbara, CA) additionally equipped with a Wavetek function generator and SRS830 lock-in amplifier. W_2C-coated tips ($l \approx 125$ μm, resonant frequency approximately 350 kHz) were used. The piezoresponse image was collected as a phase (θ) signal from the lock-in amplifier. A polished ceramic specimen of $Li_{1.1}Nb_{0.9}Ti_{0.1}O_3$ was the primary composition used for the experiments.

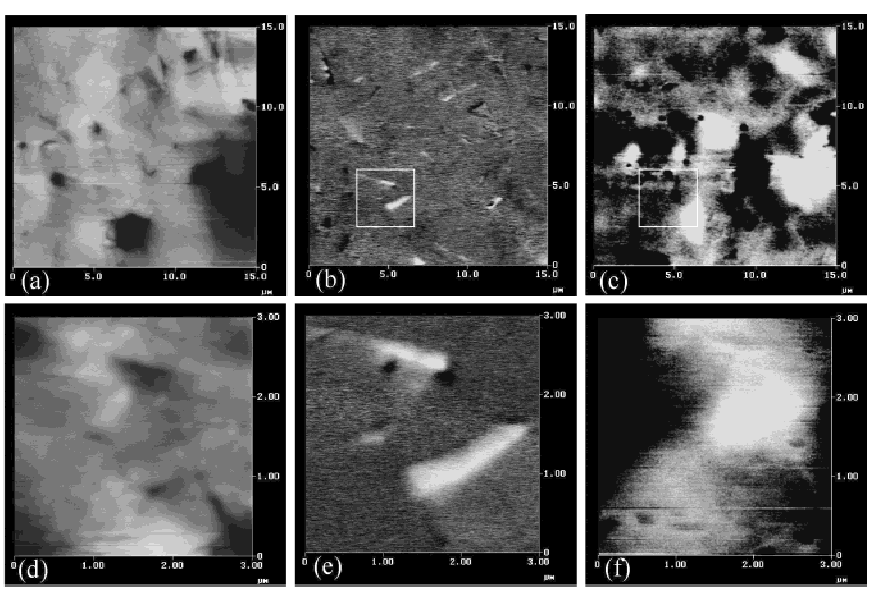

FIG. 2. (a) Topographical, (b) piezoresponse, and (c) surface potential images of the surface of $Li_{1.1}Nb_{0.9}Ti_{0.1}O_3$ ceramics. (d)–(f) show magnified images of the region in a white frame.

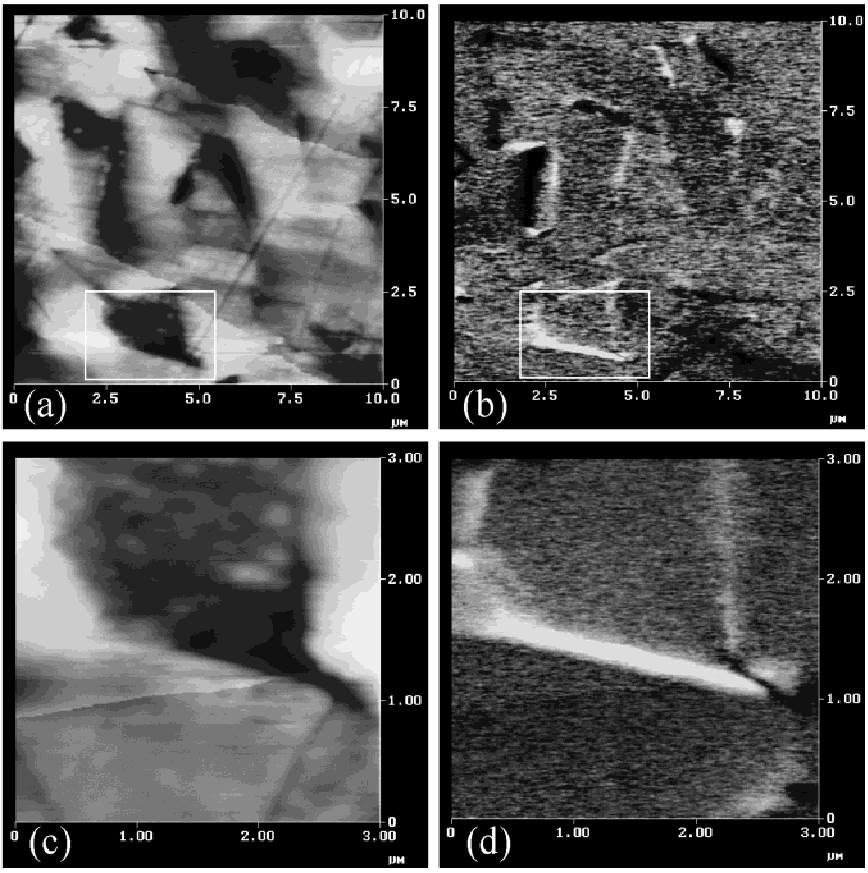

FIG. 3. (a) Topographical and (b) piezoresponse images of the surface of $Li_{1.1}Nb_{0.9}Ti_{0.1}O_3$ ceramics. (c) and (d) show magnified images of the region in a white frame.

Shown in Figs. 2(a)–2(c) is a 15-μm scan of a region on the $Li_{1.1}Nb_{0.9}Ti_{0.1}O_3$ surface in (a) topographical, (b) piezoresponse, and (c) surface potential modes. PRI clearly demonstrates a small number of light and dark elongated features on an otherwise uniform background; large topographic features result only in minor "ripples." At the same time, the SSPM image contains a number of large scale potential variations that can be attributed to topographic artifacts, work-function offsets between grains with different orientations, surface contaminants, etc. Figures 2(d)–2(f) represent the magnified images of the region shown in the white frame. It can be clearly seen that two pronounced features on the piezoresponse image correspond to a grain boundary on the topographical image.

This point can be further illustrated by another set of topographic and piezoresponse images acquired at different scan sizes shown on Fig. 3. It is evident that the dark and light features are located at the boundaries of hexagonal grains, while nothing can be seen at platelike grain boundaries. The width of the inclusions is typically 100–300 nm, though smaller features are seen as well. This observation implies that piezoactive inclusions are located at the grain boundaries and the ferroelectric axis is oriented along the hexagonal *c*-axis, which is characteristic of $LiNbO_3$.

In conclusion, for the first time we have applied the piezoresponse imaging technique to investigate a multiphase system. This unique method allowed us to demonstrate the presence of the second phase and analyze the phase distribution and microstructure of the sample, which could not be analyzed by other techniques due to the similar structural and chemical characteristics of both phases. These experiments suggest that piezoresponse imaging can be applied for the studies of composites, inhomogeneous ferroelectrics, and other multiphase objects.

REFERENCES

1. M.E. Villafuerte-Castrejon, A. Aragon-Pina, R. Valenzuela, and A.R. West, J. Solid State Chem. **71,** 103 (1987).
2. A. Borisevich and P.K. Davies, J. Eur. Ceram. Soc. (2001, in press).
3. R.I. Smith and A.R. West, Mater. Res. Bull. **27,** 277 (1992).

4. H. Hayasi, H. Nakano, K. Suzumura, K. Urabe, and A.R. West in *Fourth Euro Ceramics Vol. 2: Basic Science—Developments in processing of advanced ceramics—Part II*, edited by C. Galassi (Gruppo Editoriale Faenza Editrice S.p.A., Faenza, Italy, 1995), p. 391.
5. R.S. Roth and K.L. Davis, in *ACerS Ann. Meet, 89th* (The American Ceramic Society, Westerville, OH, 1987), p. 88; also in *Phase Equilibria Diagrams: Volume XI*, edited by R.S. Roth (The American Ceramic Society, Westerville, OH, 1995), p. 231.
6. P. Bordet, C. Bougerol-Chaillout, I. Grey, J.L. Hodeau, and O. Isnard, J. Solid State Chem. **152,** 546 (2000).
7. *Landolt-Bornstein New Series*, edited by K-H. Hellwege and A.M. Hellwege (Springer-Verlag, Berlin, Germany, 1981), Vol. 16a, p. 90.
8. A. Efimov and S.R. Cohen, J. Vac. Sci. Tech. A **18,** 1051 (2000).
9. K. Franke, H. Huelz, and M. Weihnacht, Surf. Sci. **415,** 178 (1998).
10. G. Zavala, J.H. Fendler, and S. Trolier-McKinstry, J. Appl. Phys. **81,** 7480 (1997).
11. A. Gruverman, O. Auciello, and H. Tokumoto, Annu. Rev. Mater. Sci. **28,** 101 (1998).
12. C. Durkan, M.E. Welland, D.P. Chu, and P. Migliorato, Phys. Rev. B **60,** 16198 (1999).
13. L.M. Eng, J. Fousek, and P. Gunter, Ferroelectrics **191,** 211 (1997).
14. *Command reference manual* (Digital Instruments, Santa Barbara, CA, 1997).